Contemporary Engineering Sciences, Vol. 8, 2015, no. 18, 799 - 807
HIKARI Ltd, www.m-hikari.com
http://dx.doi.org/10.12988/ces.2015.57204

Simulation of the Railway under Dynamic Loading.

Part 1. Ray Method for Dynamic Problem

Alexey A. Loktev

Moscow State University of Civil Engineering (MGSU)
26, Yaroslavskoe shosse, Moscow, 129337, Russian Federation

Ekaterina A. Gridasova

Far Eastern Federal University (FEFU)
8, Sukhanova st., Vladivostok, 690001, Russian Federation

Evgeniya V. Zapol'nova

Moscow State University of Railway Engineering (MSURE)
22/2, Chasovaya st., Moscow, 125993, Russian Federation

Abstract

This paper is concerned with the modelling of the railway behaviour under dynamic load from a wheelset taking into account elastic, visco-elastic and elastoplastic properties of the interaction area between two solid bodies. Moreover, the influence of elastic anisotropic properties of the embankment, which differ in three main directions: along rails, along sleepers and vertically downward is investigated. The wave equations of the railway allow one to suggest that deformation of both the track structure and the embankment outside of the contact area is based on propagation of the final-velocity wave surfaces. From the described in the present paper scheme it can be concluded that the main magnitudes, i.e., magnitudes defining mainly the type of a quasi-volume wave and dynamic behavior of construction of the top railway are obtained by solving the differential equations, whereas the accompanying magnitudes are obtained by solving the algebraic equations.

Keywords: Dynamic interaction, Condition of compatibility, Railway embankment, Ray method, Boundary conditions, Intervals of the ray series

1 Introduction

In order to explore in detail the process of dynamic loading of the track structure with subsequent establishment of dependencies for sags and stresses it is necessary to simulate the dependencies of the force of interaction on different types of deformation (including crushing deformation) [1-10]. The main approaches that allow the detailed modelling of the interaction process between two rigid bodies differ from one another in the force acting in the contact area [1-5] and the nature of motion of the rail points outside of the interaction region [6-13].

The force of the interaction of two bodies can be described by the Hertz equation. According to experimental and theoretical investigations this approach is valid when the initial velocity of the interaction between bodies is rather low (less or equal to 5 m/s), i.e., the crushing of the rail material occurs in a quasi-static way and the transverse shear wave in the plate propagates either with infinite velocity [2, 11, 12] or with finite velocity [2, 5, 6, 13].

In this paper, the problems associated with dynamic interaction of a solid body with a planar structure are addressed by using the wave theory, which is based on the propagation of the wave surfaces of strong and weak discontinuities in the contacting target [5, 6, 14]. As a method of analysis, the ray method suggested by Achenbach and Reddy [7] and further developed for dynamic contact cases in references [2, 6] is used.

After the beginning of the interaction of the wheelset, which is represented as a solid body and a construction of the top railway, the contact area with the radius of r_0 is formed in this construction and both the quasi-longitudinal and quasi-transverse waves, which fronts represent surfaces of strong discontinuity, start to propagate from its surface. In a two-dimensional element, surfaces of strong discontinuity represent cylindrical surfaces-stripes, which generator lines are parallel to the normal to the middle surface, i.e., axis *z*, whereas the guiding lines, which are located in the middle plane, represent circles expanding with normal velocities $G^{(\alpha)}$ (the index α defines the wave number, 1 – corresponds to the longitudinal wave and 2 - to the transverse wave).

2 Governing equations

The embankment of the railway is modelled by an elastic orthotropic two-dimensional Uflyand-Mindlin element that exhibits a cylindrical anisotropy. In the polar coordinate system, the dynamic behaviour of this element is described using equations that take into account the rotary inertia of the cross sections, deformation of the transverse shear and axial symmetry of the problem:

$$D_r\left(\frac{\partial^2\varphi}{\partial r^2}+\frac{1}{r}\frac{\partial\varphi}{\partial r}\right)-D_\theta\frac{\varphi}{r^2}+hKG_{rz}\left(\frac{\partial w}{\partial r}-\varphi\right)=-\rho\frac{h^3}{12}\frac{\partial^2\varphi}{\partial t^2}, \qquad (1)$$

$$KG_{rz}\left(\frac{\partial^2 w}{\partial r^2}-\frac{\partial \varphi}{\partial r}\right)+KG_{rz}\frac{1}{r}\left(\frac{\partial w}{\partial r}-\varphi\right)=\rho\frac{\partial^2 w}{\partial t^2}, \tag{2}$$

$$C_r\left(\frac{\partial^2 u}{\partial r^2}+\frac{1}{r}\frac{\partial u}{\partial r}\right)-C_\theta\frac{u}{r^2}=\rho h\frac{\partial^2 u}{\partial t^2}, \tag{3}$$

$$C_k\left(\frac{\partial^2 v}{\partial r^2}+\frac{1}{r}\frac{\partial v}{\partial r}-\frac{v}{r^2}\right)=\rho h\frac{\partial^2 v}{\partial t^2}, \tag{4}$$

$$D_k\left(\frac{\partial^2 \psi}{\partial r^2}+\frac{1}{r}\frac{\partial \psi}{\partial r}-\frac{\psi}{r^2}\right)-KhG_{\theta z}\psi=-\rho\frac{h^3}{12}\frac{\partial^2 \psi}{\partial t^2}. \tag{5}$$

where $D_r=\frac{h^3}{12}B_r, D_\theta=\frac{h^3}{12}B_\theta, D_k=\frac{h^3}{12}B_k, C_r=hB_r, C_\theta=hB_\theta, C_k=hB_k$, $D_{r\theta}=D_r\sigma_\theta+2D_k$, $B_r=\frac{E_r}{1-\sigma_r\sigma_\theta}$, $B_\theta=\frac{E_\theta}{1-\sigma_r\sigma_\theta}$, $B_k=G_{r\theta}$, $E_r\sigma_r=E_\theta\sigma_\theta$, $K=\frac{5}{6}$, D_r, D_θ and C_r, C_θ - the bending rigidity and tension-compression rigidity for r and θ directions, respectively; D_k –the torsional rigidity; C_k – the shear stiffness; E_r, E_θ and σ_r, σ_θ - the elasticity coefficient and Poisson's ratio for r and θ directions, respectively; G_{rz}, $G_{\theta z}$ – the shear modulus for rz and θz planes, respectively; $w(r,\theta)$ – the normal displacement of the median surface, $u(r,\theta)$ and $v(r,\theta)$ – the tangential displacements of the median surface with respect to r and θ coordinates; $\varphi(r,\theta)$ and $\psi(r,\theta)$ – the rotation angles of the normals in r and θ directions.

In order to determine the contact force and the dynamic buckling it is necessary to find the transverse displacement $w(t)$, which is the part of the equation systems (1) and (2). The other equations represent independent subsystems, which can be solved separate from each other. The functions that can be determined from expressions (3) – (5) do not influence the investigated dynamic characteristics, that is why further only the equation systems (1) and (2) will be considered.

3 Solution method for the wave problem

For the determination of the unknown displacements in Eqs. (1) – (5), the following series expansion may be used:

$$Z(s,t)=\sum_{k=o}^{\infty}\frac{1}{k!}\left[Z_{,(k)}\right]_{t=s/G}\left(t-\frac{s}{G}\right)^k H\left(t-\frac{s}{G}\right), \tag{6}$$

where Z – the required function, $Z_{,(k)}={}^kZ/t^k$, $\left[Z_{,(k)}\right]=Z^{+}_{,(k)}-Z^{-}_{,(k)}$, the upper indices «+» and «-» of the derivative $Z_{,(k)}$ indicate that the value is found in front of and behind the

wave surface, respectively, G – the normal velocity of the wave, $H(t\text{-}s/G)$ – the Heaviside step function, s – the arc length, measured along the ray, t – time.

The proposed method is based on the geometric and kinematic conditions of compatibility, suggested in reference [1] and developed for physical components in [2] as follows

$$G\left[\frac{\partial Z_{\gamma(k)}}{\partial s}\right] = -\left[Z_{\gamma(k+1)}\right] + \frac{\delta\left[Z_{\gamma(k)}\right]}{\delta t}, \tag{7}$$

where $\delta/\delta t$ - δ - time-derivative at the surface of the wavefront.

In order to determine the coefficients of the series (6) for required functions it is necessary to differentiate the wave equations (1) – (5) k times with respect to time, calculate their difference at different sides of the wave surface and apply the compatibility condition (7). As a result, using motion equations (1) and (2) the system of recurrent differential equations is obtained. By solving this equation system the discontinuities of the desired values within the accuracy of arbitrary constants [5,6] are found:

$$\left(1-\frac{\rho G^2}{B_r}\right)\omega_{\varphi(k+1)} = 2\frac{\delta\omega_{\varphi(k)}}{\delta t} + Gr^{-1}\omega_{\varphi(k)} + b_r G X_{w(k)} + F_{\varphi(k-1)}, \tag{8}$$

$$\left(1-\frac{\rho G^2}{KG_{rz}}\right)X_{w(k+1)} = 2\frac{\delta X_{w(k)}}{\delta t} + Gr^{-1}X_{w(k)} - G\omega_{\varphi(k)} + F_{w(k-1)}, \tag{9}$$

where $X_{w(k)} = \left[w_{,(k+1)}\right]$, $\omega_{\varphi(k)} = \left[\varphi_{,(k+1)}\right]$, $b_r = hKG_{rz}D_r^{-1}$, $r = r_0 + Gt$,

$$F_{\varphi(k-1)} = -\frac{\delta^2\omega_{\varphi(k-1)}}{\delta t^2} - Gr^{-1}\frac{\delta\omega_{\varphi(k-1)}}{\delta t} + G^2r^{-2}\frac{E_\theta}{E_r}\omega_{\varphi(k-1)} - b_rG\frac{\delta X_{w(k-1)}}{\delta t} + b_rG^2\omega_{\varphi(k-1)},$$

$$F_{w(k-1)} = -\frac{\delta^2 X_{w(k-1)}}{\delta t^2} - Gr^{-1}\frac{\delta X_{w(k-1)}}{\delta t} + G\frac{\delta\omega_{\varphi(k-1)}}{\delta t} + G^2r^{-1}\omega_{\varphi(k-1)}.$$

During the derivation of Eqs. (8) and (9) the axial symmetry of the problem and hence independence of the wave characteristics of the angle φ was considered. Let us further take into account only five terms of the series for unknown functions, which allows for their determination with the required accuracy. Considering k = -1, 0, 1, 2, 3 in Eqs. (8) and (9), the jumps of the corresponding order on the first and the second waves can be obtained. Setting k = -1, from Eqs. (8) and (9) on the first quasi-longitudinal wave one has

$$\rho G^{(1)2} = B_r, \quad X^{(1)}_{w(0)} = 0, \omega^{(1)}_{\varphi(0)} \neq 0, \tag{10}$$

and on the second quasi-transverse wave

$$\rho G^{(2)2} = KG_{rz}, \quad \omega^{(2)}_{\varphi(0)} = 0, X^{(2)}_{w(0)} \neq 0. \tag{11}$$

Integrating Eq. (8) at $k = 0$ one has

$$\omega_{\varphi(0)}^{(1)} = c_0^{(1)} r_1^{-1/2}, \tag{12}$$

and from Eq. (9) the following algebraic expression may be written

$$X_{w(1)}^{(1)} = -\left(G^{(1)} / f_r\right) c_0^{(1)} r_1^{-1/2}, \tag{13}$$

where $f_r = 1 - B_r / KG_{rz} = 1 - G^{(1)2} / G^{(2)2} < 0$, $1/e_r = 1 - 1/f_r$, $c_0^{(1)}$ - the arbitrary constant, $r_\alpha = G^{(\alpha)} t + r_0$ ($\alpha = 1, 2$).

After the substitution of the expressions for $X_{w(1)}^{(1)}$ and $\omega_{\varphi(0)}^{(1)}$ into Eqs. (8) and (9) at $k = 1$, the jumps $\omega_{\varphi(1)}^{(1)}$ and $X_{w(2)}^{(1)}$ are given by

$$\omega_{\varphi(1)}^{(1)} = c_1^{(1)} r_1^{-1/2} + \frac{1}{2}\left(\frac{E_\theta}{E_r} - \frac{1}{4}\right) G^{(1)} c_0^{(1)} r_1^{-3/2} - \frac{1}{2} G^{(1)} \frac{b_r}{e_r} c_0^{(1)} r_1^{1/2}, \tag{14}$$

$$X_{w(2)}^{(1)} = -\frac{G^{(1)}}{f_r}\left[c_1^{(1)} r_1^{-1/2} + \frac{1}{2}\left(\frac{E_\theta}{E_r} - \frac{5}{4}\right) G^{(1)} c_0^{(1)} r_1^{-3/2} - \frac{1}{2} G^{(1)} \frac{b_r}{e_r} c_0^{(1)} r_1^{1/2} \right], \tag{15}$$

where $c_1^{(1)}$ - the arbitrary constant, $e_r = 1 - KG_{rz} / B_r = 1 - G^{(2)2} / G^{(1)2} > 0$, at $k = 2$

$$\begin{aligned} \omega_{\varphi(2)}^{(1)} = {} & c_2^{(1)} r_1^{-1/2} + \frac{1}{2}\left(\frac{E_\theta}{E_r} - \frac{1}{4}\right) G^{(1)} c_1^{(1)} r_1^{-3/2} - \frac{1}{2} G^{(1)} \frac{b_r}{e_r} c_1^{(1)} r_1^{1/2} + \\ & + \frac{1}{8} G^{(1)2} \frac{b_r^2}{e_r^2} c_0^{(1)} r_1^{3/2} - \frac{1}{8}\left(\frac{9}{4} - \frac{E_\theta}{E_r}\right)\left(\frac{E_\theta}{E_r} - \frac{1}{4}\right) G^{(1)2} c_0^{(1)} r_1^{-5/2}, \end{aligned} \tag{16}$$

$$\begin{aligned} X_{w(3)}^{(1)} = {} & -\frac{G^{(1)}}{f_r}\left[c_2^{(1)} r_1^{-1/2} + \frac{1}{2}\left(\frac{E_\theta}{E_r} - \frac{5}{4}\right) G^{(1)} c_1^{(1)} r_1^{-3/2} - \frac{1}{2} G^{(1)} \frac{b_r}{e_r} c_1^{(1)} r_1^{1/2} - \right. \\ & - \left(\frac{E_\theta}{E_r} - 1\right) G^{(1)2} \frac{1}{f_r} c_0^{(1)} r_1^{-5/2} + \frac{1}{8}\left(\frac{E_\theta}{E_r} - \frac{1}{4}\right)^2 G^{(1)2} c_0^{(1)} r_1^{-5/2} - \\ & \left. - \left(\frac{1}{f_r} - \frac{3}{4}\right) G^{(1)2} \frac{b_r}{e_r} c_0^{(1)} r_1^{-1/2} + \frac{1}{8} G^{(1)2} \frac{b_r^2}{e_r^2} c_0^{(1)} r_1^{3/2} \right]. \end{aligned} \tag{17}$$

Similarly, on the second wave one has

at $k = 2$

$$X_{w(0)}^{(2)} = c_0^{(2)} r_2^{-1/2}, \quad \omega_{\varphi(1)}^{(2)} = G^{(2)} \frac{b_r}{e_r} c_0^{(2)} r_2^{-1/2}, \tag{18}$$

$$X_{w(1)}^{(2)} = c_1^{(2)} r_2^{-1/2} - \frac{1}{8} G^{(2)} c_0^{(2)} r_2^{-3/2} + \frac{1}{2} G^{(2)} \frac{b_r}{e_r} c_0^{(2)} r_2^{1/2}, \tag{19}$$

$$\omega_{\varphi(2)}^{(2)} = G^{(2)} \frac{b_r}{e_r} \left[c_1^{(2)} r_2^{-1/2} + \frac{3}{8} G^{(2)} c_0^{(2)} r_2^{-3/2} + \frac{1}{2} G^{(2)} \frac{b_r}{e_r} c_0^{(2)} r_2^{1/2} \right], \tag{20}$$

$$\begin{aligned} X_{w(2)}^{(2)} = {} & c_2^{(2)} r_2^{-1/2} - \frac{1}{8} G^{(2)} c_1^{(2)} r_2^{-3/2} + \frac{1}{2} \frac{b_r}{e_r} G^{(2)} c_1^{(2)} r_2^{1/2} + \\ & + \frac{1}{8} \frac{b_r^2}{e_r^2} G^{(2)2} c_0^{(2)} r_2^{3/2} + \frac{9}{128} G^{(2)2} c_0^{(2)} r_2^{-5/2}, \end{aligned} \tag{21}$$

$$\omega_{\varphi(3)}^{(2)} = G^{(2)} \frac{b_r}{e_r} \left\{ c_2^{(2)} r_2^{-1/2} + \frac{3}{8} G^{(2)} c_1^{(2)} r_2^{-3/2} + \frac{1}{2} G^{(3)} \frac{b_r}{e_r} c_1^{(2)} r_2^{1/2} + \right. \tag{22}$$

$$\left. + \frac{1}{8} \frac{b_r^2}{e_r^2} G^{(2)2} c_0^{(2)} r_2^{3/2} - \left[\frac{1}{e_r} \left(1 - \frac{E_\theta}{E_r} \right) + \frac{15}{128} \right] G^{(2)2} c_0^{(2)} r_2^{-5/2} + \left(\frac{1}{e_r} + \frac{3}{4} \right) \frac{b_r}{e_r} G^{(2)2} c_0^{(2)} r_2^{-1/2} \right\},$$

where $c_0^{(2)}$, $c_1^{(2)}$, $c_2^{(2)}$ - the arbitrary constants.

From the described scheme it can be concluded that the main magnitudes, i.e., magnitudes defining mainly the type of a quasi-volume wave are obtained by solving the differential equations, whereas the accompanying magnitudes are obtained by solving the algebraic equations. The found jumps allow one to write the expressions for the required functions W and Q_r in a view of the intervals of the ray series within the accuracy of the coefficients $c_i^{(\alpha)}$ (α = 1,2) (i=0,1,…4), which are determined from the boundary conditions

$$W \cong \sum_{\alpha=1}^{2} \sum_{k=0}^{4} \frac{1}{k!} X_{w(k)}^{(\alpha)} \left(y_\alpha \right)^k H\left(y_\alpha \right), \tag{23}$$

$$Q_r \cong K G_{rz} h \sum_{\alpha=1}^{2} \sum_{k=0}^{4} \frac{1}{k!} \left(-X_{w(k)}^{(\alpha)} G^{(\alpha)-1} + \frac{\delta X_{w(k-1)}^{(\alpha)}}{\delta t} G^{(\alpha)-1} - \omega_{\varphi(k-1)}^{(\alpha)} \right) \left(y_\alpha \right)^k H\left(y_\alpha \right), \tag{24}$$

where $y_\alpha = t - (r - r_0) G^{(\alpha)-1}$, magnitudes $X_{w(k)}^{(\alpha)}$, $\omega_{\varphi(k)}^{(\alpha)}$ and their δ - derivatives are calculated at y_α=0.

4 Numerical investigations and conclusions

Figure 1 shows dependencies of the dimensionless dynamic sag on time and the influence of the dimensionless interaction velocity (which is the corrected value of

the vehicle displacement velocity) $\tilde{V}$ on the value of the railway embankment subsidence with orthotropic properties is investigated: curve 1 is obtained for $\tilde{V}$ = $10 \cdot 10^{-3}$ (approx.150 km/h), curve 2 - $\tilde{V}$ = $8 \cdot 10^{-3}$ (approx. 120 km/h), curve 3 - $\tilde{V}$ = $6 \cdot 10^{-3}$ (approx. 90 km/h), curve 4 - $\tilde{V}$ = $4 \cdot 10^{-3}$ (approx. 60 km/h), curve 5 - $\tilde{V}$ = $2 \cdot 10^{-3}$ (approx.40 km/h). For the calculation of the graphical dependencies the following parameters were used: E_θ / E_r =0.75, $\tilde{m}$ =25, $G^{(2)} / G^{(1)}$ =0.349, $\tilde{h}$ =1, $\tilde{E}$ =$1.1 \cdot 10^{-6}$. The obtained sag values may be compared to the threshold limit value, which is determined from regulatory documentation. In Fig. 1 this threshold limit value is shown by the horizontal line. For the given parameters of the construction $\tilde{f}_n$ =0.06 and it is seen that at $\tilde{V}$ higher than a certain value $\tilde{V}_{cr}$, the sag exceeds the regulatory value, and the rigidity condition is not fulfilled.

The conducted investigations have shown that the operating by a kinematic parameter (sag) it is possible to find such a velocity of the travelling train, at which the railroad would be less destroyed. On the contrary, by knowing the parameters of the velocity one can determine the suitable materials for the embankment and the underlayer, as well as the parameters of reinforcement of the road base, at which the arising sags and stresses would not exceed the acceptable value.

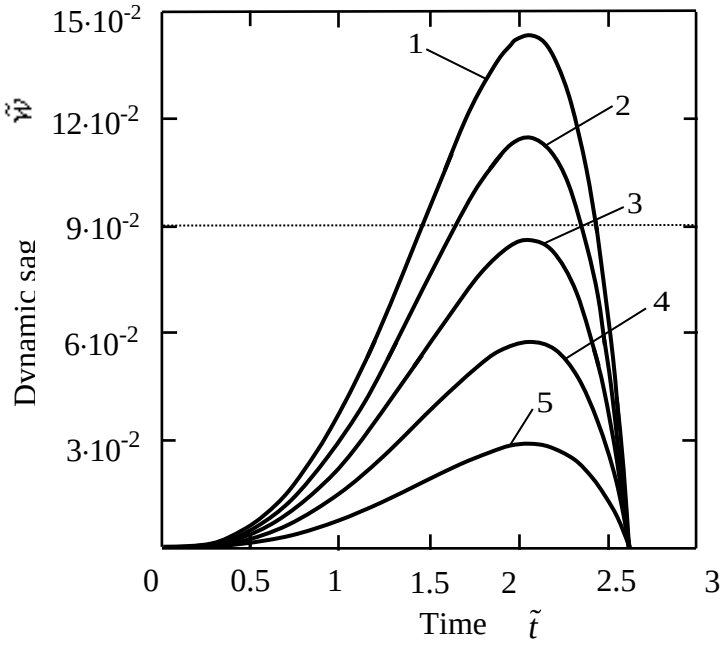

Fig. 1 Time dependencies of the dynamic sag for different values of the dimensionless initial velocity of interaction $\tilde{V}$

References

[1] T.Y. Thomas, *Plastic Flow and Fracture in Solids.* N.Y.; L.:Acad. Press, 1961.

[2] Yu.A. Rossikhin, M.V. Shitikova, A ray method of solving problems connected with a shock interaction, *Acta Mechanica*, **102** (1994), no. 1-4, 103 - 121. http://dx.doi.org/10.1007/bf01178521

[3] A.A. Loktev, Non-elastic models of interaction of an impactor and an Uflyand–Mindlin Plate, *International Journal of Engineering Science*, **50** (2012), no. 1, 46 - 55. http://dx.doi.org/10.1016/j.ijengsci.2011.09.004

[3] A.A. Loktev, Dynamic contact of a spherical indenter and a prestressed orthotropic Uflyand-Mindlin plate, *Acta Mechanica* **222** (2011), no. 1-2, 17 - 25. http://dx.doi.org/10.1007/s00707-011-0517-8

[4] D.G. Birukov, I.G. Kadomtsev, Elasto-plastic non-axisymmetric impact of a parabolic body upon a spherical shell [Uprugo-plasticheskii neosesimmetrichnii udar papabolicheskogo tela po sfericheskoi obolochke], *Prikl Mekh Tekh Fiz*, 46(1), (2005), 181-186 (in Russian).

[5] A.A. Loktev, E. A. Gridasova, V.V. Kramchaninov, The Method of Determining the locations of reinforcing elements in a composite orthotropic plate undergoing dynamic impact. Part 1. Wave problem, *Applied Mathematical Sciences*, **9** (2015), no. 71, 3533 - 3540. http://dx.doi.org/10.12988/ams.2015.52180

[6] A.A. Loktev, E. A. Gridasova, V.V. Kramchaninov, R.N. Stepanov, The Method of Determining the locations of reinforcing elements in a composite orthotropic plate undergoing dynamic impact. Part 2. Calculation Algorithm, *Applied Mathematical Sciences*, **9** (2015), no. 71, 3541 - 3547. http://dx.doi.org/10.12988/ams.2015.53252

[7] J.D. Achenbach, D.P. Reddy, Note on wave propagation in linear viscoelastic media, *Z. Angew. Math. Phys.*, **18** (1967), 141 - 144. http://dx.doi.org/10.1007/bf01593905

[8] S. Abrate, Modelling of impact on composite structures, *Compos Struct*., **51** (2001), 129 - 138. http://dx.doi.org/10.1016/s0263-8223(00)00138-0

[9] R. Olsson, M.V. Donadon , B.G. Falzon, Delamination threshold load for dynamic impact on plates, *International Journal of Solids and Structures*, **43** (2006), 3124 - 3141. http://dx.doi.org/10.1016/j.ijsolstr.2005.05.005

[10] R. Tiberkak, M. Bachene, S. Rechak, B. Necib, Damage prediction in composite plates subjected to low velocity impact, *Compos Struct.*, **83** (2008), 73 - 82. http://dx.doi.org/10.1016/j.compstruct.2007.03.007

[11] M. Agostinacchio, D. Ciampa, M. Diomedi, S. Olita, Parametrical analysis of the railways dynamic response at high speed moving loads, *Journal of Modern Transportation*, **21** (2013), no. 3, 169 - 181. http://dx.doi.org/10.1007/s40534-013-0022-y

[12] M. Fang, S.F. Cerdas, Ya. Qiu, Numerical determination for optimal location of sub-track asphalt layer in high-speed rails, *Journal Modern Transp.*, **21** (2013), no. 2, 103 - 110. http://dx.doi.org/10.1007/s40534-013-0012-0

[13] Yu.N. Mazov, A.A. Loktev, V.P. Sychev, Evaluation of the influence of defects of the wheels of the rolling stock on the railway tracks [Otsenka vliyaniya defektov koles podvizhnogo sostava na sostoyaniya zheleznodorozhnogo puti], *Vestnik MGSU*, **5**, (2015), 61-72 (in Russian).

[14] A.A. Loktev, V.F. Bakhtin, I.Yu. Chernikov, D.A. Loktev, The method of determining an external defect structures by analyzing a series of images in the monitoring system [Metodika opredeleniya vneshnih defektov sooruzheniya putem analiza ego izobraghenii v sisteme monitoringa], *Vestnik MGSU*, **3**, (2015), 7-16 (in Russian).

Received: July 25, 2015; Published: September 1, 2015